Досліджені особливості зміни і балансування аеродинамічної незрівноваженості робочого колеса осьового вентилятора типу ВО-06-300 (Україна).

Знайдена аеродинамічна неврівноваженість робочого колеса, викликана установкою однієї лопатки:

– під іншим кутом атаки;

– з порушенням рівномірності кроку;

– не перпендикулярно до подовжньої осі робочого колеса;

– за наявністю відразу всіх трьох вище названих похибок встановлення.

Оцінена зміна аеродинамічної незрівноваженості від зміни густини повітря. Оцінений вплив температури повітря, висоти над рівнем моря, атмосферного тиску на густину повітря і аеродинамічну незрівноваженість.

Встановлено, що при іншому куті атаки і при порушенні перпендикулярності виникає динамічна незрівноваженість, у якій моментна складова на порядок більша за статичну складову. При порушенні рівномірності кроку виникає тільки статична складова, що лежить у площині робочого колеса.

Серед розглянутих похибок найбільш небажаною є встановлення лопатки під іншим кутом атаки. При такій похибці аеродинамічна незрівноваженість у 6–8 разів більша, ніж при інших.

При зміні в робочому колесі кута атаки однієї лопатки на $\pm 4^{o}$ можна погіршити точність балансування робочого колеса до класу точності G 6,3 при частоті 1500 об/хв, чи G 16 – при 3000 об/хв.

Встановлено, що звичайну і аеродинамічну незрівноваженості можна балансувати одночасно. Балансування доцільно проводити динамічне в двох площинах корекції. Балансування можна проводити корегуванням мас чи пасивними автобалансирами.

На конкретному прикладі показана методика врахування аеродинамічної неврівноваженості в диференціальних рівняннях руху осьового вентилятора. Відповідно до методики складові аеродинамічної незрівноваженості додаються до відповідних складових звичайної незрівноваженості.

Одержані результати застосовні на етапах проектування і виготовлення осьових вентиляторів низького тиску. Їх застосування дозволить поліпшити вібраційні характеристики зазначених вентиляторів

Ключові слова: осьовий вентилятор, аеродинамічні сили, аеродинамічна незрівноваженість, динамічне балансування, автобалансир, автобалансування

UDC 62-752+62-755 : 621.634
DOI: 10.15587/1729-4061.2018.133105

PATTERNS IN CHANGE AND BALANCING OF AERODYNAMIC IMBALANCE OF THE LOW-PRESSURE AXIAL FAN IMPELLER

L. Olijnichenko
Engineer*
E-mail: loga_lubov@ukr.net
G. Filimonikhin
Doctor of Technical Sciences, Professor, Head of Department**
E-mail: filimonikhin@ukr.net
A. Nevdakha
PhD**
E-mail: aunevdaha@ukr.net
V. Pirogov
PhD, Senior Lecturer**
E-mail: pirogovvv@ukr.net
*Department of Materials Science and Foundry***
Department of Machine Parts and Applied Mechanics*
***Central Ukrainian National Technical University
Universytetskyi ave., 8,
Kropyvnytskyi, Ukraine, 25006

1. Introduction

Axial fans are widely used in industry and in everyday life [1–2]. Reduction of noise and vibration during operation of axial fans is a relevant scientific and technical task [3–16]. Ordinary and aerodynamic (gas-dynamic) imbalances of the fan impellers are the main source of vibrations in fan machines [3–8]. The noise and vibrations of fans are also influenced by the geometry of blades [9–13].

At present, ordinary imbalance of the rotors are is rather well studied; effective techniques for its balancing have been developed. Aerodynamic imbalance has almost not been investigated theoretically.

It should be noted that the aerodynamic imbalance is modeled and calculated differently for axial fans of high [4–7] and low [14–16] pressure.

Here we shall examine aerodynamic imbalance of axial low-pressure fans using fans of the type VO 06-300/VO-12-300 (Ukraine, Russia) as an example [2]. These fans have one impeller with 3 to 5 blades. They lack a directing vane.

Underlying the research are the results of studies [14–19], classic methods of axial fans aerodynamics [20] and the

theory of air screw [21, 22], certain facts related to changing weather conditions [23], atmospheric physics [24].

2. Literature review and problem statement

Paper [3] shows that the main source of vibrations in axial fans is the ordinary imbalance of rotating parts in assembly and the aerodynamic imbalance. The latter arises from imprecisely manufactured impellers, blades, due to the difference in gaps between blade crowns and casing, etc.

Gas (air) in the high-pressure fans is compressible, which is why it is appropriate to consider the imbalance to be gas-dynamic. Gas in such fans passes under high pressure impellers, directing vanes, labyrinths of seals, etc. [4–7]. That explains the complex character of the occurrence of gas-dynamic imbalance as it depends not only on the aerodynamic characteristics of the blades, but on the mechanism of their interaction with other parts of the fan. The patterns in the emergence of a gas-dynamic imbalance in turbo assemblies of internal combustion engines were examined in [4]; paper [5] calculated a given imbalance. The features and causes of the occurrence of a gas-dynamic imbalance in gas-turbine engines were considered in [6]; paper [7] modeled this imbalance. It was established in [4–7] that the gas-dynamic imbalance is essentially dependent on air density (temperature, altitude above sea level) and can depend on the rotor speed, specifically due to the deformations of blades [6].

Air is almost not compressed in the low-pressure fans. If there is only one impeller and there is no a directing vane, the aerodynamic imbalance and noise of the fan are determined mainly by the aerodynamic characteristics of blades. Papers [9–13] investigated and optimized separate blades. Authors of [9] studied the impact of through openings in a blade on the noise of the fan. In [10], authors optimized the shape of blades in order to improve performance and reduce mass. Paper [11] reported construction of a method for the rapid optimization of impellers in axial fans and its verification. Authors of [12], in order to parametrically optimize geometrical parameters of the blade, applied an algorithm of object optimization. Paper [13] presented a procedure for choosing the design of the impeller (air screw), aimed at experimental verification. The cited studies do not examine the ordinary and aerodynamic imbalance of the impeller.

Aerodynamic imbalance and aerodynamic forces acting on the blades of a low-pressure axial fan were investigated in papers [14–16]. In [14], authors established an analogy between the ordinary and aerodynamic imbalances. They have proven a possibility for the simultaneous balancing of these imbalances by rotor mass correction or via passive auto-balancers. It was established that the aerodynamic imbalance is directly proportional to air density and therefore varies depending on weather conditions and the operating conditions of a fan. Paper [15] determined the principal vector and moment of aerodynamic forces acting on the fan rotary impeller. Authors of [15] built a mathematical model for the static balancing of the impeller of axial fan using an automatic ball balancer.

Dynamic balancing of the fan by two passive auto-balancers was studied in paper [17] – in theory, in [18] – experimentally, in [19] – using 3D computer simulation of dynamics.

The above overview reveals that it is necessary to examine how separate blades of a low-pressure fan create aerodynamic imbalance. It is required to estimate the magnitude of a given imbalance, the patterns of change, and a procedure to account for the fan in the differential equations of motion. It is also necessary to prepare recommendations addressing the balancing of aerodynamic imbalance.

3. The aim and objectives of the study

The aim of present research is to devise a procedure for determining and estimating the magnitude of aerodynamic imbalance of the impeller in axial fan. Achieving this aim would make it possible to determine and assess the magnitudes of aerodynamic imbalances, to take into consideration aerodynamic imbalances in the differential equations of the fan motion.

To accomplish the aim, the following tasks have been set:

– to devise a procedure for calculating the aerodynamic imbalance caused by an inaccurate mounting of one blade to the impeller;

– to establish the magnitude of aerodynamic imbalance for different air density;

– to devise recommendations on the balancing of the ordinary and aerodynamic imbalances by rotor mass correction and using passive auto-balancers;

– to devise recommendations and to give an example of accounting for the aerodynamic imbalance in differential equations of the axial fan motion.

4. Methods of research into the patterns of change and balancing of aerodynamic imbalance

4. 1. Balancing scheme of the composite rotor and causes for the occurrence of aerodynamic imbalance

Balancing scheme of the composite rotor. The composite rotor is dynamically balanced (in two correction planes P_1, P_2) (Fig. 1) [14]. It is created by the rotating parts of the fan – an electric motor rotor, an impeller mounted onto the rotor, etc. If the composite rotor is balanced by auto-balancers, their casings also relate to it.

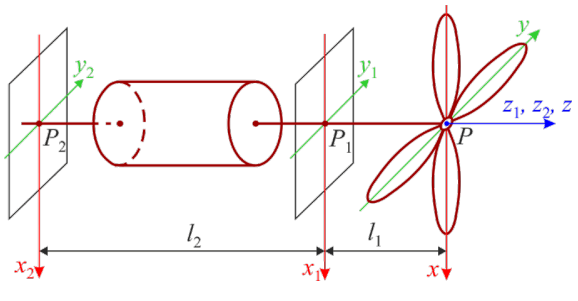

Fig. 1. Schematic of dynamic balancing of the composite rotor [14]

The composite rotor rotates around its own longitudinal axis in still air (gas) with a constant angular velocity ω. Aerodynamic imbalance is determined relative to the axes, rigidly connected to the rotor, shown in Fig. 1.

Causes for the occurrence of aerodynamic imbalance taken into consideration. The impeller has $n \geq 3$ blades arranged in a circle with equal step $\Delta\theta = 2\pi/n$ (Fig. 1). Manufacturers of the axial fans VO 06-300 make blades according to a single pattern. The blades are almost identical geometrically.

The impeller is mounted onto the shaft of electric motor with a minimum eccentricity and skewness. Most errors in the manufacture of an impeller occur at the imprecise placement of blades.

Without limiting the generality, we shall assume that only one blade, number j, is installed in the impeller with errors. We shall consider the following cases:

– the angle of attack of the blade differs from the angles of attack of other blades;

– the blade deflects from the perpendicular to the longitudinal axis of the fan;

– the blade is installed in the impeller so that it violates step $\Delta\theta$;

– the blade is mounted to the impeller with all the three above errors.

Aerodynamic imbalance depends on air density [14]. We shall take into consideration that air density depends on [24]:

– atmospheric pressure;

– air temperature;

– altitude above sea level, and almost does not depend on air humidity [24].

4. 2. Components of the aerodynamic forces that create aerodynamic imbalance, reduced to two correction planes

The principal vector and moment of aerodynamic forces [14]. Because the impeller is fabricated with a defect, the principal vector **R** and the principal moment of aerodynamic forces $\mathbf{M}_P$, reduced to point P, have components R_x, R_y, transverse to the longitudinal rotor axis (Fig. 2, *a*) and M_x, M_y (Fig. 2, *b*). These components form the aerodynamic imbalance and can deflect the longitudinal axis of the rotor from the rotation axis both translationally and rotationally.

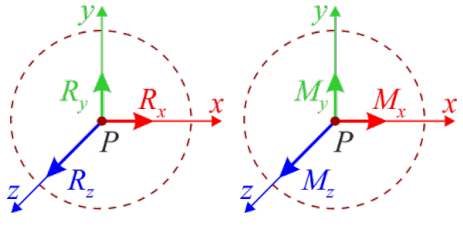

a *b*

Fig. 2. Reducing the aerodynamic forces to [14]: *a* – principal vector; *b* – principal moment

The component force R_z is formed by the air moved by its blades along the longitudinal axis of the impeller. The component moment M_z prevents the rotation of the impeller. It is overcome by the torque from the fan engine.

Reduced aerodynamic forces [14]. Fig. 3 shows forces A_{1x}, A_{1y}, A_{2x}, A_{2y}, which are in the correction planes and are statically equivalent to components R_x, R_y, M_x, M_y.

Projections of the reduced aerodynamic forces onto the x, y axes [14]:

$$A_{1x}=\frac{M_y+(l_1+l_2)R_x}{l_2},\quad A_{1y}=\frac{-M_x+(l_1+l_2)R_y}{l_2},$$

$$A_{2x}=-\frac{M_y+l_1R_x}{l_2},\quad A_{2y}=\frac{M_x-l_1R_y}{l_2}. \qquad (1)$$

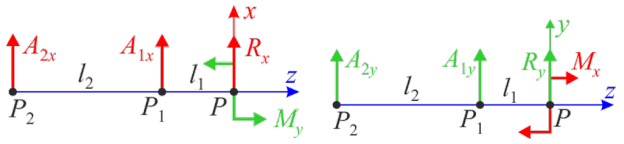

a *b*

Fig. 3. Reducing the components of aerodynamic forces that form the imbalance to two planes of correction [14]: *a* – xPz plane; *b* – yPz plane

Note that these forces do not balance aerodynamic forces and are statically equivalent to them.

4. 3. Patterns in determining the aerodynamic forces

We apply an approximated theory of air screw in the form of totality n of wings with finite span [21, 22].

According to the theory, the aerodynamic forces acting on blade number i are reduced to the resultant $\mathbf{R}_i$ (Fig. 4). The resultant is in the characteristic cross-section of the blade, located at distance r_i from the rotation axis (Fig. 4, *a*). The resultant is applied to the center of pressure of the profile (Fig. 4, *b*).

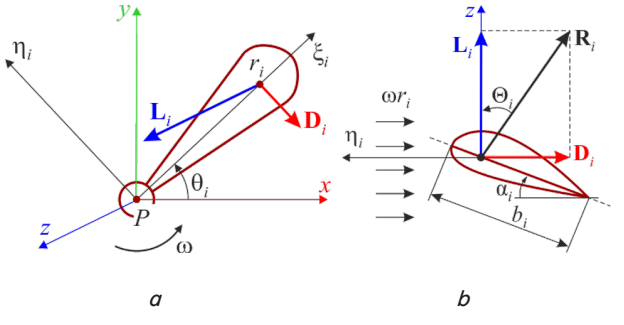

a *b*

Fig. 4. The resultant $\mathbf{R}_i$ of aerodynamic forces acting on blade number i: *a* – action on the blade; *b* – location in the characteristic cross-section of the blade

The resultant has two components. The first component $\mathbf{L}_i$ is the lifting force

$$L_i=\frac{1}{2}\rho C_{zi}A_i r_i^2\omega^2,\quad /i=\overline{1,n}/, \qquad (2)$$

where C_{zi} is the coefficient of the lifting force; ρ is the air density; A_i is the area of the characteristic cross-section of the blade; r_i is the distance between the longitudinal axis of the impeller to the characteristic cross-section of the blade (approximately 70 % of the radius of the impeller).

The second component $\mathbf{D}_i$ is the drag force

$$D_i=\frac{1}{2}\rho C_{\eta i}A_i r_i^2\omega^2,\quad /i=\overline{1,n}/, \qquad (3)$$

where $C_{\eta i}$ is the coefficient of drag force.

If all blades are the same, then

$$D_i=D=\frac{1}{2}\rho C_\eta A_b r^2\omega^2,$$

$$L_i=L=\frac{1}{2}\rho C_z A_b r^2\omega^2,\quad /i=\overline{1,n}/, \qquad (4)$$

and projections of the principal vector and the principal moment of aerodynamic forces onto the *Pxyz* axes:

$$R_x = 0,\ \ R_y = 0,\ \ R_z = nL = \frac{1}{2}n\rho C_z A r^2\omega^2,$$

$$M_x = 0,\ \ M_y = 0,\ \ M_z = -nDr = -\frac{1}{2}n\rho C_\eta A r^3\omega^2. \qquad (5)$$

In this case, the aerodynamic imbalance is absent.

If only one blade, number *j*, is installed imprecisely (with a defect), then for it

$$D_j = D + \Delta D_j,\ \ L_j = L + \Delta L_j, \qquad (6)$$

where ΔL_j is a change in the lifting force; ΔD_j is a change in the drag force.

Projections of the principal vector and the principal moment of aerodynamic forces on the *x*, *y* axes:

$$R_x = \Delta D_j \sin\theta_j,\ \ R_y = -\Delta D_j \cos\theta_j,$$

$$M_x = r\Delta L_j \sin\theta_j,\ \ M_y = -r\Delta L_j \cos\theta_j. \qquad (7)$$

These projections create aerodynamic imbalance.

This model is applicable for determining the aerodynamic imbalance that occurs when installing one blade: at another angle of attack; in violation of the uniformity of the step.

In order to examine the case when the blade is not perpendicular to the longitudinal axis of the impeller, the approximated theory of air screw is to be modified.

5. Research results

5. 1. Calculation of basic characteristics of the fan

Technical specifications of the examined fans can be found at the web sites of manufacturers (for example, ChP "Gradvent", Kharkiv, Ukraine: http://gradvent.org.ua) [2].

Table 1 gives technical specifications and the calculated characteristics of axial fans VO-06-300 (VO-12-300). Characteristics were calculated based on the parameters for the rated operating mode of the fan. The fans were operated at a change in air temperature in the range of –40÷+40 °C (up to +50 °C at a short operating time).

Table 1

Characteristics of axial fans VO-06-300 (VO-12-300)

Fan No.	*N*, rpm	*w*, rad/s	*d*, m	*r*, m	p_v, N/m^2	A_b, m^2	C_z	C_h
3.15	1,500	157.08	0.315	0.110	50	0.00866	0.834	0.077
	3,000	314.16			220		0.917	0.093
4	1,500	157.08	0.4	0.140	72	0.01396	0.744	0.062
	3,000	314.16			297		0.768	0.065
5	1,500	157.08	0.5	0.175	114	0.02182	0.754	0.063
6.3	1,000	104.72	0.63	0.2205	76	0.03464	0.713	0.056
	1,500	157.08			181		0.754	0.063
8	1,000	104.72	0.8	0.280	104	0.05585	0.605	0.041
	1,500	157.08			247		0.638	0.045
10	1,000	104.72	1.0	0.350	173	0.08727	0.644	0.046
12.5	750	78.54	1.25	0.4375	156	0.13635	0.661	0.048
	1,000	104.72			259.5		0.618	0.042

In Table 1:

N – number of impeller revolutions per minute;

ω – angular rotation velocity of the impeller;

d – diameter of the disk, which creates the impeller;

r – distance from the axis of rotation of the impeller to the characteristic cross-section of the blade;

p_v – full pressure at the rated operating mode of the fan;

C_z – coefficient of the blade's lifting force;

C_η – coefficient of the blade's drag force.

Basic characteristics of the fan were calculated in the following order.

1. Area of the disk, which creates the impeller, m^2:

$$A_d = \pi d^2 / 4.$$

2. Lifting force acting on the disk in general, N:

$$L_d = p_v A_d.$$

3. Lifting force acting on a single blade, N:

$$L_0 = L_d / n.$$

4. Area of the single blade, m^2:

$$A_b = A_d f_b / n,$$

where f_b is a part of the area of the disk onto which the impeller is projected, $0<f_b<1$.

5. Angular frequency of rotation of the composite rotor, rad/s:

$$\omega = \pi N / 30.$$

6. Coefficient of the lifting force:

$$C_z = \frac{2L_0}{\rho_0 A_b r^2\omega^2},$$

where ρ_0=1.2 kg/m^3 is the density of air under normal conditions.

7. Coefficient of elongation of the blade

$$\lambda = d^2 / (4A_b).$$

8. Coefficient of the drag force:

$$C_\eta \approx C_z^2 / (\pi\lambda).$$

The calculations were carried out at n=3, f_b=1/3, r=0.7R. The characteristics given in Table 1 are required to assess the aerodynamic imbalance caused by the incorrect installation of the blade.

5. 2. Determining the aerodynamic imbalance when installing one blade with a different angle of attack

5. 2. 1. Sequence of calculations

Let all the blades, except one (number *j*), be mounted on the impeller at the same angle of attack. Let the angle of attack of blade number *j* be different by angle χ from the angles of attack of other blades.

Let for the sake of certainty a blade with a defect be in the position in which angle θ_j=90°. We find then, from (8), such projections of the principal vector and

the principal moment of aerodynamic forces onto the x, y axes:

$$R_x = \Delta D_j, \quad R_y = 0, \quad M_x = r\Delta L_j, \quad M_y = 0. \tag{8}$$

Substituting the obtained projections (8) in equation (1), we derive projections of the reduced aerodynamic forces onto the x, y axes:

$$A_{1x} = \frac{(l_1 + l_2)\Delta D_j}{l_2}, \quad A_{1y} = -\frac{r\Delta L_j}{l_2},$$

$$A_{2x} = -\frac{l_1\Delta D_j}{l_2}, \quad A_{2y} = \frac{r\Delta L_j}{l_2}. \tag{9}$$

A change in the lifting force and drag force acting on the defective blade:

$$\Delta L_j = \frac{1}{2}\rho\Delta C_{zj}A_b r^2\omega^2,$$

$$\Delta D_j = \frac{1}{2}\rho\Delta C_{\eta_j}A_b r^2\omega^2, \tag{10}$$

where ΔC_{zj} is the change, for the defective blade, in magnitude C_z, and $\Delta C_{\eta j}$ – in magnitude C_η.

The blade is flown over at small subsonic speeds. Air can be considered perfect, non-compressible. Coefficients C_z, C_η depend on the profile of the blade and the angle of attack. For almost flat blades [21]

$$C_z \approx 2\pi(\alpha - \alpha_0) = 2\pi\alpha_A, \tag{11}$$

where α is the angle of attack, α_0 is the angle of null lifting force, $\alpha_A = \alpha - \alpha_0$ is the aerodynamic angle of attack.

For the case of an almost elliptical blade with a finite span [21]:

$$C_\eta \approx C_z^2 / (\pi\lambda), \tag{12}$$

where λ is the coefficient of the blade elongation. It equals

$$\lambda = l^2 / A_b, \tag{13}$$

where $l \approx d/2$ is the blade span.

For the imprecisely mounted blade

$$C_{zj}(\chi) = C_z + \Delta C_{zj}(\chi) =$$
$$= 2\pi(\alpha_A + \chi) = 2\pi\alpha_A + 2\pi\chi = C_z + 2\pi\chi,$$

$$C_{\eta j}(\chi) = C_\eta + \Delta C_{\eta j}(\chi) \approx \frac{C_{zj}^2(\chi)}{\pi\lambda} =$$
$$= \frac{C_z^2 + 4C_z\pi\chi + 4\pi^2\chi^2}{\pi\lambda} \approx \frac{C_z^2}{\pi\lambda} + \frac{4C_z}{\lambda}\chi = C_\eta + \frac{4C_z}{\lambda}\chi.$$

Hence

$$\Delta C_{zj}(\chi) = 2\pi\chi, \quad \Delta C_{\eta j}(\chi) = \frac{4C_z}{\lambda}\chi. \tag{14}$$

Absolute changes in the lifting and drag forces

$$\Delta L_j(\chi) = \frac{1}{2}\rho\Delta C_{zj}(\chi)\cdot A_b r^2\omega^2,$$

$$\Delta D_j(\chi) = \frac{1}{2}\rho\Delta C_{\eta j}(\chi)\cdot A_b r^2\omega^2. \tag{15}$$

The calculations are performed in the following order.

1. Change the coefficients of lifting and drag forces acting on the defective blade

$$\Delta C_{zj}(\chi) = 2\pi\chi, \quad \Delta C_{\eta j}(\chi) = \frac{4C_z}{\lambda}\chi.$$

2. Absolute changes in the lifting force (ΔL_j)) and drag force (ΔD_j), which act on the defective blade (number j) as a function of absolute change in the angle of attack (χ), kg×m/s^2:

$$\Delta L_j(\chi) = \frac{1}{2}\rho\Delta C_{zj}(\chi)\cdot A_b r^2\omega^2,$$

$$\Delta D_j(\chi) = \frac{1}{2}\rho\Delta C_{\eta j}(\chi)\cdot A_b r^2\omega^2.$$

3. Projections of the reduced aerodynamic forces onto the x, y axes, kg×m/s^2:

$$A_{1x}(\chi) = \frac{(l_1 + l_2)\Delta D_j(\chi)}{l_2}, \quad A_{1y}(\chi) = -\frac{r\Delta L_j(\chi)}{l_2},$$

$$A_{2x}(\chi) = -\frac{l_1\Delta D_j(\chi)}{l_2}, \quad A_{2y}(\chi) = \frac{r\Delta L_j(\chi)}{l_2}.$$

4. Projections of the aerodynamic imbalances formed by the defective blade in correction planes onto the x, y axes, g×mm:

$$S_{1x}(\chi) = \frac{A_{1x}(\chi)}{\omega^2}\cdot 10^6, \quad S_{1y}(\chi) = \frac{A_{1y}(\chi)}{\omega^2}\cdot 10^6,$$

$$S_{2x}(\chi) = \frac{A_{2x}(\chi)}{\omega^2}\cdot 10^6, \quad S_{2y}(\chi) = \frac{A_{2y}(\chi)}{\omega^2}\cdot 10^6. \tag{16}$$

5. Modules of the imbalances formed by the defective blade in correction planes, g×mm:

$$S_1(\chi) = \sqrt{S_{1x}^2(\chi) + S_{1y}^2(\chi)},$$

$$S_2(\chi) = \sqrt{S_{2x}^2(\chi) + S_{2y}^2(\chi)}. \tag{17}$$

6. Vibration speed of point P_i, located along the longitudinal axis of the rotor in correction plane number i=1, 2:

$$V_{P_i}(\chi) = S_i(\chi)\frac{\omega}{m_\Sigma}\cdot 10^{-3}, \quad i = 1,2,$$

where m_Σ is the mass of the composite rotor (the total mass of rotating parts of the fan). Moreover, the greater the speed of rotation of the composite rotor and the larger its length, the more precise the formulae.

5. 2. 2. Calculation results

1. The calculations were carried out for the fan VO 06-300 No. 4 at N=1,500 rpm and N=3,000 rpm. Basic parameters of the fan are given in Table 1. Other parameters: m_Σ=2.5 kg; l_1=0 m (the first plane of correction coincides with the plane of the impeller); l_2=0.28 m.

Table 2 gives the calculated reduced aerodynamic imbalances depending on air density.

Table 2

Dependence of the reduced aerodynamic imbalances on air density

ρ, kg/m³	N, rpm	$S_i(\chi)$, g×mm							
		±1°		±2°		±3°		±4°	
		imp.	shank	imp.	shank	imp.	shank	imp.	shank
0.8	1,500	6.32	6.00	12.64	12.00	18.97	18.01	25.29	24.01
	3,000	6.34	6.00	12.68	12.00	19.03	18.01	25.37	24.01
1.2	1,500	9.48	9.00	18.97	18.01	28.45	27.01	37.93	36.01
	3,000	9.51	9.00	19.03	18.01	28.54	27.01	38.05	36.01
1.6	1,500	12.64	12.00	25.29	24.01	37.93	36.01	50.58	48.02
	3,000	12.68	12.00	25.37	24.01	38.05	36.01	50.74	48.02

Table 2 shows that:

– aerodynamic imbalances (almost) do not depend on the speed of rotation of the impeller that testifies to the correctness of the devised procedure;

– the greater the density of the air, the larger the imbalances in the respective planes of correction;

– an increase in the deviation from the angle of attack of the defective blade leads to an increase in the magnitudes of imbalances.

The magnitudes of vibration speeds at points P_1, P_2 are given in Table 3.

Table 3

Dependence of magnitudes of vibration speeds at points P_1, P_2 on air density

ρ, kg/m³	N, rpm	$V_{Pi}(\chi)$, mm/s							
		±1°		±2°		±3°		±4°	
		imp.	shank	imp.	shank	imp.	shank	imp.	shank
0.8	1,500	0.397	0.377	0.794	0.754	1.192	1.131	1.589	1.509
	3,000	0.797	0.754	1.594	1.509	2.391	2.263	3.188	3.017
1.2	1,500	0.596	0.566	1.192	1.131	1.788	1.697	2.383	2.263
	3,000	1.195	1.131	2.391	2.263	3.586	3.394	4.782	4.526
1.6	1,500	0.794	0.754	1.589	1.509	2.383	2.263	3.178	3.017
	3,000	1.594	1.509	3.188	3.017	4.782	4.526	6.376	6.034

Table 3 shows that an increase in the frequency of rotation of the impeller by 2 times leads to an (almost) 2-time increase in the vibration speeds of control points P_1, P_2, which testifies to the correctness of the devised procedure.

One can also see that at the largest air density and the deviation in the angle of attack of the defective blade:

– ±1° the impeller would be imbalanced in line with the accuracy class G 1 (International standard ISO 21940-11:2016 (Mechanical vibration – Rotor balancing – Part 11: Procedures and tolerances for rotors with rigid behavior)) at N=1,500 rpm, or G 2.5 at N=3,000 rpm;

– ±2° the impeller would be imbalanced in line with the accuracy class G 2.5 at N=1,500 rpm, or G 6.5 at N=3,000 rpm;

– ±4° the impeller would be imbalanced in line with the accuracy class G 6.3 at N=1,500 rpm, or G 16 at N=3,000 rpm.

Calculations are carried out similarly for other fans. However, the obtained similar results (are not given in this paper).

As the first plane of correction coincides with the plane of the impeller, l_1=0 and

$$A_{1x}(\chi)=\Delta D_j(\chi),\quad A_{1y}(\chi)=-r\Delta L_j(\chi)/l_2,$$

$$A_{2x}(\chi)=0,\quad A_{2y}(\chi)=r\Delta L_j(\chi)/l_2.$$

Thus, for the case under consideration, aerodynamic forces create a dynamic imbalance. Calculations show that $\Delta L_j(\chi)>>\Delta D_j(\chi)$. Component $\Delta L_j(\chi)$ forms a pure moment imbalance. Therefore, this dynamic imbalance can be balanced only dynamically – in two planes of correction.

5. 3. Aerodynamic imbalance for the case when the blade perpendicularity to the axis of rotation is broken

5. 3. 1. Sequence of calculations

Let blade number j be mounted not perpendicularly to the longitudinal axis of the impeller (Fig. 5). The angle between the blade and the perpendicular to the longitudinal axis is denoted by δ.

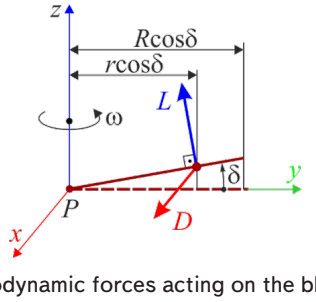

Fig. 5. Aerodynamic forces acting on the blade when it is mounted with a violation of the perpendicularity to the longitudinal axis of the impeller

We find from Fig. 5 the following projections of the principal vector and the principal moment of aerodynamic forces onto the x, y axes:

$$R_x=0,\quad R_y=-L\sin\delta\approx-L\delta,\quad M_x=0,\quad M_y=0. \qquad (18)$$

Substituting the derived projections in equation (1), we shall obtain projections of the reduced aerodynamic forces onto the x, y axes:

$$A_{1x}=0,\quad A_{1y}=-(l_1+l_2)L\delta/l_2,$$

$$A_{2x}=0,\quad A_{2y}=l_1L\delta/l_2. \qquad (19)$$

Further sequence of calculation is obvious and it is therefore not given.

5. 3. 2. Calculation results

Table 4 gives the calculated reduced aerodynamic imbalance $S_1(\delta)$ and vibration speed $V_{P1}(\delta)$ of point P_1 depending on air density.

Relationship between the magnitudes, obtained at N=1,500 rpm and N=3,000 rpm, once again confirm correctness of the constructed procedure.

Table 4

Dependence of the reduced imbalance and vibration speed of point P_1 on air density

ρ, kg/m^3	N, rpm	$S_1(\delta)$, g×mm; $V_{P1}(\delta)$, mm/s							
		±1°		±2°		±3°		±4°	
		S_1	V_{P1}	S_1	V_{P1}	S_1	V_{P1}	S_1	V_{P1}
0.8	1,500	1.422	0.089	2.844	0.179	4.265	0.268	5.684	0.357
	3,000	1.467	0.184	2.933	0.369	4.398	0.553	5.862	0.737
1.2	1,500	2.133	0.134	4.266	0.268	6.397	0.402	8.526	0.536
	3,000	2.200	0.276	4.399	0.553	6.597	0.829	8.793	1.105
1.6	1,500	2.844	0.179	5.688	0.357	8.529	0.536	11.369	0.714
	3,000	2.933	0.369	5.865	0.737	8.796	1.105	11.724	1.473

Table 4 shows that at the largest air density of air and a deviation of the blade from the perpendicular to the longitudinal axis of the fan at ±4° the impeller acquires imbalance:

– at N=1,500 rpm, in line with the accuracy class G 1;

– at N=3,000 rpm, in line with the accuracy class G 2,5.

Non-perpendicular mounting of the blade forms imbalances and vibrations that are almost 4 times less than mounting the blade with another angle of attack.

In the examined case, with respect to l_1=0

$$A_{1x}=0,\quad A_{1y}=-L\delta,\quad A_{2x}=0,\quad A_{2y}=0.$$

Thus, a defective blade creates pure static imbalance in the plane of the impeller. Therefore, it must be balanced statically in the impeller plane.

5. 4. Aerodynamic imbalance when the step of mounting a blade is violated

5. 4. 1. Sequence of calculations

Let blade number j be deflected at angle γ from the required angular position in the impeller (Fig. 6).

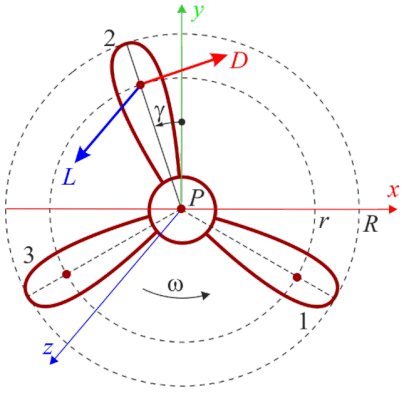

Fig. 6. Aerodynamic forces acting on a blade when it is mounted with an angular error

We find form Fig. 6 the following projections of the principal vector and the principal moment of aerodynamic forces onto the x, y axes:

$$R_x=0,\quad R_y=D\sin\gamma\approx D\gamma,$$

$$M_x=0,\quad M_y=Lr\sin\gamma\approx Lr\gamma. \qquad (20)$$

Substituting the derived projections in equation (1), we obtain projections of the reduced aerodynamic forces onto the x, y axes:

$$A_{1x}=Lr\gamma/l_2,\quad A_{1y}=(l_1+l_2)D\gamma/l_2,$$

$$A_{2x}=-Lr\gamma/l_2,\quad A_{2y}=-l_1D\gamma/l_2. \qquad (21)$$

Further sequence of calculations is obvious and it is therefore not given.

5. 4. 2. Calculation results

Table 5 gives the calculated reduced aerodynamic imbalances depending on air density.

Table 5

Dependence of the reduced imbalances on air density

ρ, kg/m^3	N, rpm	$S_i(\gamma)$, g×mm							
		±1°		±2°		±3°		±4°	
		imp.	shank	imp.	shank	imp.	shank	imp.	shank
0.8	1,500	0.721	0.711	1.442	1.442	2.162	2.133	2.883	2.844
	3,000	0.744	0.733	1.488	1.467	2.232	2.200	2.976	2.933
1.2	1,500	1.081	1.067	2.162	2.133	3.243	3.200	4.325	4.267
	3,000	1.116	1.100	2.232	2.200	3.348	3.300	4.464	4.400
1.6	1,500	1.422	1.422	2.883	2.844	4.325	4.267	5.766	5.689
	3,000	1.488	1.467	2.976	2.933	4.464	4.400	5.951	5.867

The magnitudes of vibration speeds at points P_1, P_2 are given in Table 6.

Table 6

Dependence of magnitudes of vibration speeds at points P_1, P_2 on air density

ρ, kg/m^3	N, rpm	$V_{Pi}(\gamma)$, mm/s							
		±1°		±2°		±3°		±4°	
		imp.	shank	imp.	shank	imp.	shank	imp.	shank
0.8	1,500	0.045	0.045	0.091	0.089	0.136	0.134	0.181	0.179
	3,000	0.093	0.092	0.187	0.184	0.280	0.276	0.374	0.369
1.2	1,500	0.068	0.067	0.136	0.134	0.202	0.201	0.272	0.268
	3,000	0.140	0.138	0.280	0.276	0.421	0.415	0.561	0.553
1.6	1,500	0.091	0.089	0.181	0.179	0.272	0.268	0.362	0.357
	3,000	0.187	0.184	0.374	0.369	0.561	0.553	0.748	0.737

Table 6 shows that:

– at the largest air density and a deviation of the blade at ±4° the impeller acquires imbalance in line with the accuracy class G 0.4 at N=1,500 rpm, and G 1 at N=3,000 rpm;

– mounting the blade with a deviation from step creates imbalances and vibrations that are almost 8 times smaller than mounting the blade with another angle of attack.

In the considered case, with respect to l_1=0

$$A_{1x} = Lr\gamma / l_2, \quad A_{1y} = D\gamma,$$

$$A_{2x} = -Lr\gamma / l_2, \quad A_{2y} = 0.$$

Thus, when the uniformity of blades arrangement is violated, there occurs the dynamic imbalance. Because $D<<L$, the greatest contribution to the dynamic imbalance is provided by the moment imbalance created by the component **L**. Therefore, it is advisable to balance such an imbalance dynamically – in two correction planes.

5. 5. General case of mounting a blade with errors

Let only blade number j be mounted imprecisely among all the blades, and angles χ, γ, δ in this case are not equal to zero. Note that angles χ, γ, δ (in radians) are the magnitudes of a first-order smallness. That is why with an accuracy to the magnitudes of a first-order smallness inclusive the reduced aerodynamic forces are the sum of the respective forces that arise from each error in mounting a separate blade:

$$A_{1x}(\chi,\gamma,\delta) = [(l_1+l_2)\Delta D_j(\chi) + Lr\gamma] / l_2,$$

$$A_{1y}(\chi,\gamma,\delta) = -[r\Delta L_j(\chi) + (l_1+l_2)L\delta - (l_1+l_2)D\gamma] / l_2,$$

$$A_{2x}(\chi,\gamma,\delta) = -[l_1\Delta D_j(\chi) + Lr\gamma] / l_2,$$

$$A_{2y}(\chi,\gamma,\delta) = [r\Delta L_j(\chi) + l_1(L\delta - D\gamma)] / l_2. \qquad (22)$$

If the first plane of correction coincides with the plane of the impeller, then l_1=0 and projections of the reduced aerodynamic forces onto the x, y axes

$$A_{1x}(\chi,\gamma,\delta) = \Delta D_j(\chi) + Lr\gamma / l_2,$$

$$A_{1y}(\chi,\gamma,\delta) = -L\delta + D\gamma - r\Delta L_j(\chi) / l_2,$$

$$A_{2x}(\chi,\gamma,\delta) = -Lr\gamma / l_2,$$

$$A_{2y}(\chi,\gamma,\delta) = r\Delta L_j(\chi) / l_2. \qquad (23)$$

Projections of aerodynamic imbalances onto the x, y axes are derived from formulae (17).

Note that in the general case the total aerodynamic imbalance is dynamic in which the moment component is greater than the static component.

5. 6. Dependence of air density on atmospheric pressure, air temperature, altitude above sea level

Atmospheric pressure decreases due to increasing altitude above sea level and varies depending on weather conditions.

The largest registered atmospheric pressure on the Earth's surface, reduced to the sea level, is 108.56 kPa, the smallest being 85 kPa [23]. Thus, for a particular area, a daily, monthly, yearly change of atmospheric pressure does not exceed 24 kPa. At a normal temperature of 20 °C and a humidity of 50 % at a change in the atmospheric pressure in the range from 85÷109 kPa, air density varies in the range of 1.009÷1.296 kg/m^3 (by 1.28 times) [24].

At normal atmospheric pressure (101.34 kPa) and normal humidity (50 %), at a change in air temperature in the range of –40÷+50 °C (a temperature range that permits operation of the fan), air density in the range of 1.515÷÷1.093 kg/m^3 (by 1.39 times) [24].

At normal temperature (20 °C) and humidity (50 %), at a change in the altitude above sea level in the range from –1,000 m to 4,000 m, air density varies in the range of 1.376÷0.819 kg/m^3 (by 1.68 times) [24].

Altitude above sea level during operation of the fan does not change. That is why the causes of change in air density and aerodynamic imbalance in the operation of the fan is the change in atmospheric pressure and temperature.

Air temperature undergoes the greatest change over 24 hours. Therefore, this change will most affect a change in air density and aerodynamic imbalance.

5. 7. Procedure for taking into consideration the aerodynamic imbalance in differential equations of motion of the fan

5. 7. 1. Differential equations of motion of a two-support rotor disregarding the aerodynamic forces

Fig. 7 shows a circuit that explains motion of the rotor on a rigid weightless shaft and elastic supports [17]. Fig. 7, *a* shows position of the stationary rotor. The motion of the rotor is described relative to the immobile right rectangular coordinate system $Kx_Ky_Kz_K$. It originates in the center of masses of the motionless rotor. The z axis is directed along the axis of rotation. Similar $Guvw$ axes are rigidly connected to the rotor. In the original position, the $Guvw$ axes coincide with the $Kx_Ky_Kz_K$.

Coordinates x, y set the translational motion of the rotor together with the center of masses – point G (Fig. 7, *b*). Angles α, β define a rotation of the rotor longitudinal axis around point G (Fig. 7, *c*). The rotor rotates around the longitudinal axis at constant angular velocity ω. Rotation angle of the rotor around this axis is $\varphi=\omega t$, where t is the time.

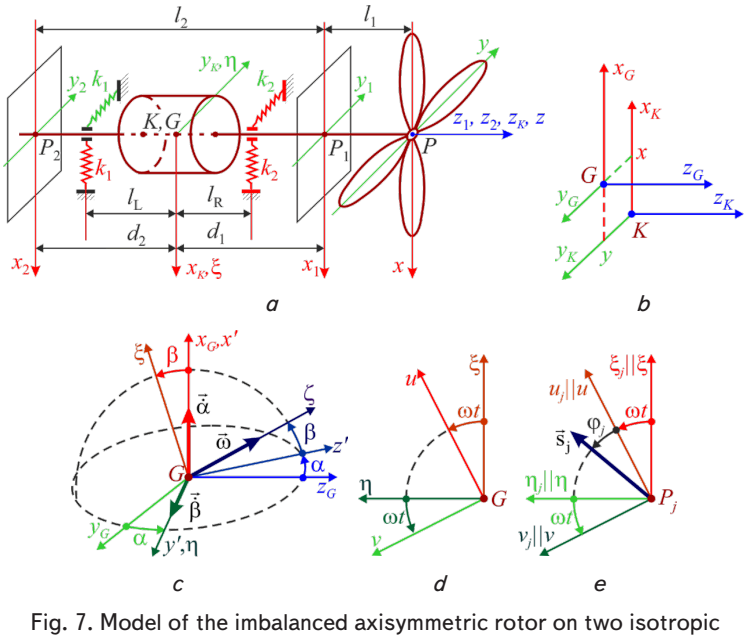

Fig. 7. Model of the imbalanced axisymmetric rotor on two isotropic elastic supports [17]: *a* – circuit of the rotor with application points of ordinary imbalances to the longitudinal axis of the rotor; *b* – translational displacement of rotor together with the center of masses *G*; *c* – rotations of the rotor longitudinal axis around the center of masses; *d* – rotor rotation around the longitudinal axis at angle ωt; *e* – rotation of ordinary imbalance $\mathbf{S}_j$, /*j*=1.2/ together with the rotor

Axial moments of inertia of the rotor relative to the principal central axes ξ_G, η_G, ζ_G, parallel to axes ξ, η, ζ (and axes u_G, v_G, w_G, parallel to axes u, v, w) are equal to A, A, C, respectively.

Differential equations of the rotor motion disregarding the aerodynamic imbalance, for small α and β take the form [17]:

$$M\ddot{x}+k_{11}x+k_{14}\beta=\omega^2[S_1\cos(\omega t+\varphi_1)+S_2\cos(\omega t+\varphi_2)],$$

$$M\ddot{y}+k_{11}y-k_{14}\alpha=\omega^2[S_1\sin(\omega t+\varphi_1)+S_2\sin(\omega t+\varphi_2)],$$

$$A\ddot{\alpha}+C\omega\dot{\beta}+k_{33}\alpha-k_{14}y=$$
$$=-\omega^2[S_1d_1\sin(\omega t+\varphi_1)-S_2d_2\cos(\omega t+\varphi_2)],$$

$$A\ddot{\beta}-C\omega\dot{\alpha}+k_{33}\beta+k_{14}x=$$
$$=\omega^2[S_1d_1\cos(\omega t+\varphi_1)-S_2d_2\cos(\omega t+\varphi_2)], \quad (24)$$

where

$$k_{11}=k_1+k_2,\quad k_{14}=k_2l_R-k_1l_L,\quad k_{33}=k_1l_L^2+k_2l_R^2. \quad (25)$$

5. 7. 2. Taking into consideration the aerodynamic imbalance

Fig. 8 shows schematic for determining current projections of the reduced aerodynamic forces onto the x, y axes. It is considered that

$$|\alpha|,|\beta|,|\chi|,|\gamma|,|\delta|<<1.$$

Projections are determined with an accuracy to the magnitudes of a first-order smallness relative to angles α, β, χ, γ, δ. Under such conditions, projections onto the ξ, η axes coincide with the projections onto the x, y axes.

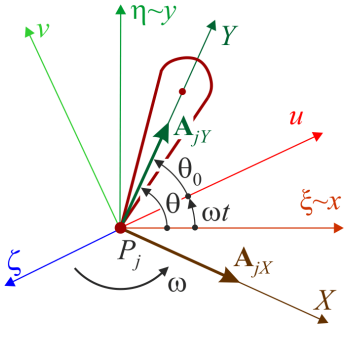

Fig. 8. Determining the projections of the reduced aerodynamic forces onto the x, y axes

The schematic shows a blade that creates the aerodynamic imbalance (without a number). It is turned relative to the u axis at angle θ_0. The blade rotates together with the composite rotor. In this case, the u axis rotates relative to the ζ axis at angle ωt (Fig. 7, *d*). Therefore, the angle that defines at time point t position of the blade relative to the ξ axis is equal to

$$\theta=\theta_0+\omega t. \quad (26)$$

Projections of the aerodynamic imbalance onto the X, Y axis are determined from equalities (22) applying a change of indexes of the axes:

$$A_{1X}(\chi,\gamma,\delta)=[(l_1+l_2)\Delta D(\chi)+Lr\gamma]/l_2,$$

$$A_{1Y}(\chi,\gamma,\delta)=-[r\Delta L(\chi)+(l_1+l_2)L\delta-(l_1+l_2)D\gamma]/l_2,$$

$$A_{2X}(\chi,\gamma,\delta)=-[l_1\Delta D(\chi)+Lr\gamma]/l_2,$$

$$A_{2Y}(\chi,\gamma,\delta)=[r\Delta L(\chi)+l_1(L\delta-D\gamma)]/l_2. \quad (27)$$

We find from Fig. 8

$$A_{jx}(\chi,\gamma,\delta,\theta_j)=A_{jX}(\chi,\gamma,\delta)\sin\theta_j+A_{jY}(\chi,\gamma,\delta)\cos\theta_j,$$

$$A_{jy}(\chi,\gamma,\delta,\theta_j)=-A_{jX}(\chi,\gamma,\delta)\cos\theta_j+A_{jY}(\chi,\gamma,\delta)\sin\theta_j,$$

$$/j=1,2/, \quad (28)$$

where index j refers to the plane of correction rather than the blade.

Projections of the reduced aerodynamic imbalances onto the x, y axes:

$$S_{jx}(\chi,\gamma,\delta,\theta_j)=A_{jx}(\chi,\gamma,\delta,\theta_j)/\omega^2,$$

$$S_{jy}(\chi,\gamma,\delta,\theta_j)=A_{jy}(\chi,\gamma,\delta,\theta_j)/\omega^2,\ /j=1,2/. \quad (29)$$

Complete imbalance of the composite rotor is the sum of ordinary and aerodynamic components:

$$s_{jx}(\chi,\gamma,\delta,\theta_j)=S_{jx}(\chi,\gamma,\delta,\theta_j)+S_j\cos(\omega t+\varphi_j),$$

$$s_{jy}(\chi,\gamma,\delta,\theta_j)=S_{jy}(\chi,\gamma,\delta,\theta_j)+S_j\sin(\omega t+\varphi_j),$$

$$/j=1,2/. \quad (30)$$

Differential equations of the rotor motion with respect to aerodynamic imbalance

$$M\ddot{x}+k_{11}x+k_{14}\beta=\omega^2[s_{1x}(\chi,\gamma,\delta,\theta_j)+s_{2x}(\chi,\gamma,\delta,\theta_j)],$$

$$M\ddot{y}+k_{11}y-k_{14}\alpha=\omega^2[s_{1y}(\chi,\gamma,\delta,\theta_j)+s_{2y}(\chi,\gamma,\delta,\theta_j)],$$

$$A\ddot{\alpha}+C\omega\dot{\beta}+k_{33}\alpha-k_{14}y=$$
$$=-\omega^2[s_{1y}(\chi,\gamma,\delta,\theta_j)d_1-s_{2y}(\chi,\gamma,\delta,\theta_j)d_2],$$

$$A\ddot{\beta}-C\omega\dot{\alpha}+k_{33}\beta+k_{14}x=$$
$$=\omega^2[s_{1x}(\chi,\gamma,\delta,\theta_j)d_1-s_{2x}(\chi,\gamma,\delta,\theta_j)d_2]. \quad (31)$$

Thus, if there is a system of differential equations of the rotor motion without the impeller, one can derive from them differential equations of the rotor motion with the impeller, which take into consideration the aerodynamic imbalance.

6. Discussion of results related to patterns in change and balancing of the aerodynamic imbalance

The developed procedure for determining and estimation of aerodynamic imbalances of the impeller of axial fan was applied for low-pressure axial fans, type VO-06-300 (VO-12-300), and others.

Aerodynamic imbalances caused by the imprecise mounting of the blade to the impeller are similar to the ordinary imbalance because:

– they are reduced to two planes of correction;

– they do not depend on the angular velocity of rotor rotation.

The magnitudes of aerodynamic imbalances, in contrast to the ordinary ones, are directly proportional to air density.

In the general case, aerodynamic imbalance is dynamic in which the moment component is an order of magnitude larger than the static one.

Among the considered errors in mounting the blade to the impeller, the most undesired is the error related to mounting the blade at another angle of attack. This error gives rise to the aerodynamic imbalance (mostly, moment), which is 6–8 times higher than the aerodynamic imbalance arising from other errors.

A ±4° change in the angle of attack of a single blade in the impeller can worsen the balancing accuracy of rotating parts in assembly to the accuracy class G 6.3 at N=1,500 rpm, or G 16 at N=3,000 rpm.

Ordinary and aerodynamic imbalance can be balanced by rotor mass correction. In this case, it is appropriate to balance dynamically in two correction planes. Balancing should be performed not under normal conditions but under conditions to which the fan will be exposed during operation. If these conditions change, it is necessary to perform balancing at a mean value of air (gas) density.

If the impeller is balanced at a certain air density, then a change in the air density will result in the occurrence and change of aerodynamic imbalance. Air density mostly changes over time and in magnitude with the change in air temperature. A change in air temperature from –40 to +50 °C (a temperature range that permits operation of the fan) may lead to a 1.4-time change in air density.

In order to reduce vibrations caused by a change in the aerodynamic imbalance, it is advisable:

– to additionally balance rotating parts in assembly, continuously, by using passive auto-balancers;

– to aerodynamically balance the impeller, separately, by eliminating the errors in blade mounting.

To account for the aerodynamic imbalance in differential equations of motion of the fan, it is necessary to add the components of aerodynamic imbalance to the respective components of ordinary imbalance.

It is possible to consider small aerodynamic forces in the differential equations of motion of the fan, which occur at small motions of the impeller's longitudinal axis. The example of such a consideration is given in [16].

The obtained theoretical results make it possible to simulate and estimate the magnitude of aerodynamic imbalance, to take into consideration the aerodynamic imbalance in the differential equations of motion. The obtained calculation results indicate that the aerodynamic imbalances, similar to the ordinary ones, is an essential source of vibrations in axial fans.

It should be noted that the results obtained are applicable only for the low-pressure axial fans with a single impeller. The results of calculations were obtained for the rated operating mode of the fan. Given the significant dependence of aerodynamic forces on the conditions of operation of the fan, the estimations obtained could not be accepted as final and need clarification or verification.

In the further research we plan to conduct computational and full-scale experiments for balancing the aerodynamic imbalance through the rotor mass correction and using passive auto-balancers.

7. Conclusions

1. We have developed a model and devised a procedure for calculating the aerodynamic imbalance caused by the imprecise mounting of one blade to the impeller. We have examined cases when a blade is mounted:

– at a different angle of attack;

– with a violation of the uniformity of the step;

– not perpendicularly to the longitudinal axis of the impeller;

– with all three of the above-mentioned errors present at once.

In all cases, aerodynamic imbalance is similar to the ordinary one because:

– they are reduced to two planes of correction;

– they do not depend on the angular velocity of rotor rotation.

The magnitudes of aerodynamic imbalances, in contrast to the ordinary ones, are directly proportional to air density.

It is established that a different angle of attack and a violation of the perpendicularity lead to the occurrence of a dynamic imbalance in which the moment component is the order of magnitude greater than the static component. A violation of the uniformity of the step gives rise exclusively to a static component, which is in the plane of the impeller.

2. Among the errors considered, the most undesired error relates to mounting a blade at a different angle of attack. At such an error the aerodynamic imbalance is 6–8 times higher than that for other errors.

A ±4° change in the angle of attack for one blade in the impeller can worsen the balancing accuracy of rotating parts in assembly to the accuracy class G 6.3 at a frequency of 1,500 rpm, or G 16 – at N=3,000 rpm.

Ordinary and aerodynamic imbalances can be balanced by rotor mass correction. In this case, it is appropriate to conduct dynamic balancing in two correction planes.

If the impeller is balanced at a certain air density, then at a different air density there will occur the aerodynamic imbalance. Air density mostly changes over time and in magnitude with the change in air temperature. When air temperature changes from –40 to +50 °C (a temperature range that permits operation of the fan), air density may change by 1.4 times.

It is recommended to prevent a change in the aerodynamic imbalance:

– by aerodynamic balancing (elimination of errors in mounting the blades);

– by continuous additional balancing of rotating parts in assembly using passive auto-balancers.

3. In order to take into consideration aerodynamic imbalance in differential equations of motion of the fan, it is necessary to add the components of aerodynamic imbalance to the respective components of the ordinary imbalance.

References

1. Polyakov V., Skvortsov L. Pumps and Fans. Moscow: Stroyizdat, 1990. 336 p.
2. Axial fans VO 06-300/VO-12-300 // Gradvent. URL: http://gradvent.org.ua/ventilyatory/ventilyatory-osevye/vo-06-300

3. Ziborov K., Vanga G., Marenko V. Imbalance As A Major Factor Influencing The Work Rotors Mine Main Fan // Modern engineering. Science and education. 2013. Issue 3. P. 734–740. URL: http://docplayer.ru/36451188-Udk-k-a-ziborov-g-k-vanzha-v-n-marenko.html
4. Korneev N. Aerodynamic disbalance of the turbocompressor as the reason of lowering of power indexes of internal combustion engines // Machine Builder. 2008. Issue 10. P. 24–27.
5. Korneev N. V., Polyakova E. V. The calculation of the aerodynamic the disbalance rotor of turbocharger ICE // Machine Builder. 2014. Issue 8. P. 13–16.
6. Idelson A. M., Kuptsov A. I. Elastic deformation of fan blades as a factor, influencing the gas-dynamic unbalance // Vestnik SSAU. 2006. Issue 2-1 (10). P. 234–238.
7. Idelson A. M. Modeling of aerodynamic unbalance on fan blades // Problems and prospects of engine development. 2003. P. 180–185.
8. Suvorov L. M. Procedure for low speed mass balancing and aerodynamics of high speed vane rotor: Pat. No. 2419773 RU. MPK G01M 1/00 (2006.01) / applicant and Suvorov L. M. No. 2009109011/28; declareted: 11.03.2009; published: 27.05.2011, Bul. No. 15.
9. Numerical simulation and experimental research on the aerodynamic performance of large marine axial flow fan with a perforated blade / Yang X., Wu C., Wen H., Zhang L. // Journal of Low Frequency Noise Vibration and Active Control. 2017. P. 1–12. doi: 10.1177/0263092317714697
10. Multi-objective genetic optimization of impeller of rail axial fan based on Kriging model / Qu X., Han X., Bi R., Tan Y. // Zhongguo Jixie Gongcheng/China Mechanical Engineering. 2015. Vol. 26, Issue 14. P. 1938–1943.
11. Bamberger K., Carolus T. Development, Application, and Validation of a Quick Optimization Method for the Class of Axial Fans // Journal of Turbomachinery. 2017. Vol. 139, Issue 11. P. 111001. doi: 10.1115/1.4036764
12. Application of the objective optimization algorithm in parametric design of impeller blade / Liu Z., Han B., Yeming L., Yeming L. // 2017. Vol. 50, Issue 1. P. 19–27. URL: http://journals.tju.edu.cn/zrb/Upload/PaperUpLoad/c3eb690d-ce15-49e7-98c4-2d431ed-f2c0d.pdf
13. Almazo D., Rodríguez C., Toledo M. Selection and Design of an Axial Flow Fan // World Academy of Science, Engineering and Technology International Journal of Aerospace and Mechanical Engineering. 2013. Vol. 7, Issue 5. P. 923–926.
14. Filimonikhin G., Olijnichenko L. Investigation of the possibility of balancing aerodynamic imbalance of the impeller of the axial fan by correction of masses // Eastern-European Journal of Enterprise Technologies. 2015. Vol. 5, Issue 7 (77). P. 30–35. doi: 10.15587/1729-4061.2015.51195
15. Filimonikhin G. B., Yatsun V. V. Determination of the principal vector and the principal moment of aerodynamic forces acting on the rotating impeller of the fan // Collection of scientific works KNTU. 2009. Issue 22. P. 364–370.
16. Yatsun V. V. A mathematical model of the self-important culmovami auto-balancers of the crank of the axis fan // Vesnik mining university. 2009. Issue 9. P. 11–18.
17. Application of the empirical criterion for the occurrence of auto-balancing for axisymmetric rotor on two isotropic elastic supports / Filimonikhin G., Filimonikhina I., Yakymenko M., Yakimenko S. // Eastern-European Journal of Enterprise Technologies. 2017. Vol. 2, Issue 7 (86). P. 51–58. doi: 10.15587/1729-4061.2017.96622
18. Experimental study of the process of the static and dynamic balancing of the axial fan impeller by ball auto-balancers / Olijnichenko L., Goncharov V., Sidei V., Horpynchenko O. // Eastern-European Journal of Enterprise Technologies. 2017. Vol. 2, Issue 1 (86). P. 42–50. doi: 10.15587/1729-4061.2017.96374
19. On the limited accuracy of balancing the axial fan impeller by automatic ball balancers / Olijnichenko L., Hruban V., Lichuk M., Pirogov V. // Eastern-European Journal of Enterprise Technologies. 2018. Vol. 1, Issue 1 (91). P. 27–35. doi: 10.15587/1729-4061.2018.123025
20. Brusylovskyy I. V. Aerodynamics of axial fans. Moscow: Engineering, 1984. 240 p.
21. Alexandrov V. L. Balloon screws. Moscow: Oborongiz, 1951. 493 p.
22. Zahordan A. M. The elementary theory of the helicopter. Moscow: Voenizdat, 1955. 216 p.
23. World Meteorological Organization Global Weather & Climate Extremes Archive // Arizona State University. URL: https://wmo.asu.edu
24. Khrgian A. Kh. Fizika atmosfery [Physics of the atmosphere]. Leningrad: Gidrometeoizdat, 1969. 476 p.